Available online at www.sciencedirect.com
SCIENCE DIRECT®
International Journal of Thermal Sciences 45 (2006) 691–696
International Journal of Thermal Sciences
www.elsevier.com/locate/ijts

Computation of transient-temperature profiles in objects exposed to simulated lightning currents

I.A. Metwally [a,b,c,*], A.A. A-Rahim [d], F. Heidler [c], W. Zischank [c]

[a] *Department of Electrical & Computer Engineering, College of Engineering, Sultan Qaboos University, Oman*
[b] *Department of Electrical Engineering, Faculty of Engineering, Mansoura University, Mansoura 35516, Egypt*
[c] *EIT 7, Faculty of Electrical Engineering, University of the Federal Armed Forces – Munich D-85577, Germany*
[d] *Department of Mechanical Engineering, Faculty of Engineering, Mansoura University, Mansoura 35516, Egypt*

Received 4 July 2005; received in revised form 12 October 2005; accepted 12 October 2005

Available online 18 November 2005

Abstract

This paper presents a theoretical analysis of transient temperature distribution in metals and composites struck by different lightning currents to simulate objects of interest, especially aircrafts. A computer program based on the finite volume technique is written to compute the transient-temperature distributions in three dimensions due to both high-amplitude impulse currents (IC) and the relatively low-amplitude long-duration currents (LDC). Typical waveform of the discharge current during lightning strikes to objects near/on ground (negative downward flash), at high altitudes (negative upward flash) and in-flight (e.g. aircrafts) are simulated with different amplitudes and durations. The simulation considers the IC as first negative, or superimposed or subsequent return strokes with respect to the LDC. Different types of metals and carbon-fiber composites are also investigated to compare their thermal transient responses. Finally, the theoretical results are verified by using a sophisticated high-speed infrared camera to measure the rear-face temperature profiles of metals as a function of the coordinates and time due to both IC and LDC.

Keywords: Heating effect; Lightning currents; Metals; Rear-face temperature; Transient temperature

1. Introduction

Lightning is one of the natural threats that must be considered for safety reasons in the design of many objects [1]. These objects are [1–3]:

(1) in-flight 'airborne' or landed aircrafts, and rockets,
(2) munitions and nuclear weapons,
(3) storage/collection tanks and pipelines of petroleum/gas industries,
(4) direct-current gas-insulated switchgear and lines, and
(5) optical ground/shielding wires.

Most of the in-flight measurements (∼90%) of lightning strikes to aircrafts are when the aircraft itself triggers a lightning discharge leading to the formation of the bi-leader phenomenon [4,5]. The rest of the in-flight measurements (∼10%) happen when the aircraft intercepts a natural lightning channel. The average probability of a lightning strike to a given aircraft is somewhere between 1000 and 20 000 flight hours [2], e.g. every civilian airliner is struck about once per year in average [4]. Therefore, the study of lightning aircraft interaction is of significant importance. When an aircraft is in the vicinity of a lightning leader, the electric field from the lightning leader will initiate connecting leaders from the body of the aircraft which intercept the lightning leader. The original lightning leader is not diverted. The interaction can occur for all types of natural lightning as intra- and inter-cloud discharges or cloud-to-ground discharges [2,6]. In addition, aircrafts often trigger the flashes themselves in regions where there are strong electric fields causing a bi-leader process starting from the aircraft itself as mentioned above [6]. One of the most dangerous lightning events is a direct strike to the tank of the aircraft. Even if there is no burn-through, the temperature rise inside of a fuel tank may exceed a critical value and the fuel may ignite and destroy the whole tank and the surroundings. Hot spots of

* Corresponding author.
E-mail address: metwally@squ.edu.om (I.A. Metwally).

1290-0729/$ – see front matter
doi:10.1016/j.ijthermalsci.2005.10.005

1 cm^2 require a temperature of greater than 800 °C to ignite [7]. Also, a 600–700 μJ spark represents a 50% ignition probability, where the minimum acceptable hazard limit of energy is 200 μJ [7].

Ground flashes can be divided into downward (cloud-to-ground) and upward (ground-to-cloud) flashes [2,8–10]. Long-duration currents (LDC) "square-like waveforms" occur in negative downward and upward ground flashes, cloud-to-cloud flashes, and aircraft- and rocket-triggered lightning. Most of the downward ground flashes (∼90%) are of negative polarity, where they normally strike ground or medium height structures (<60 m) [8–10]. These flashes are normally composed of several impulse currents (typically 3 or 4) of which the first one usually has the highest peak value of some 10 kA [8–10]. LDC of a few 100 A may flow for a duration of a few 100 ms in the lightning channel after one of these impulse currents [8–10]. This type of LDC is often referred to "continuing currents". On the other hand, very high structures usually trigger upward ground flashes, where the probability of upward lightning strikes increases with height [3]. Upward flashes are usually of negative polarity and start with an initiation LDC with or without superimposed impulse currents. Subsequent impulse currents may follow [8,10]. During the in-flight measurements [1], the aircraft or the rocket itself initiates the lightning, which contains LDC of a few 100 A and duration of a few 100 ms [1]. Therefore, it is of significant importance to study the effect of such mixed current (LDC and IC) on the transient-temperature distribution in the struck objects.

Composite materials are steadily increasing in importance as structural materials [11,12]. Carbon fiber reinforced plastics (CFRP) represent a branch of these composites. They meet the basic aims of aerospace industry such as improving in the structural efficiency with a reduced mass and without compromising structural strength [12,13]. Most solid carbon fiber composites (CFC) laminates employed as aircraft skins having thicknesses range from 2 mm to 5 mm [6]. Skins of any of these thicknesses can safely conduct lightning currents away from strike points, thus the protection design objectives are as follows:

(a) preventing hazardous damage,
(b) providing adequate lightning current paths among parts, so as to prevent damage at joints, and
(c) coordinating with other electrical requirements, e.g. lightning indirect effects.

The available types of CFC are [6]:

(1) woven wire fabrics,
(2) expanded metal foils,
(3) metal coated CFC, and
(4) interwoven wires.

The latter type achieves arc-root dispersion and the damage is limited to the outermost ply as well as its weight penalty is very small.

In this paper a computation of the three-dimension (3-D) transient temperature distribution in metals and composites struck by different lightning currents is introduced using a written computer program based on the finite volume technique. Also, the theoretical results are verified using the previously published experimental works [14,15].

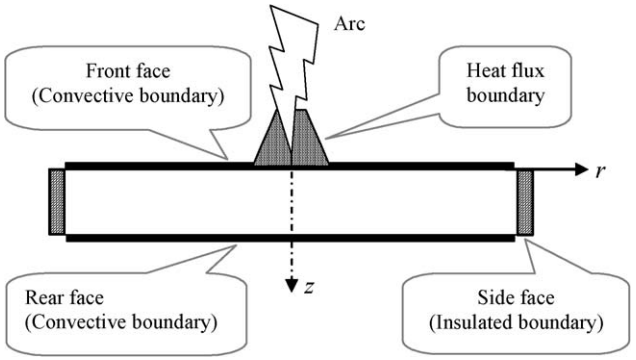

Fig. 1. Schematic of the coordinate system and the thermal boundary conditions.

2. Computer program and assumptions

The thermal effect of lightning strikes to objects can be simulated by the transient heat conduction in solids. This is governed by the energy equation in axisymmetric coordinates (r, z) for constant thermal properties as in [16]

$$\rho c \frac{\partial \vartheta}{\partial t} = k\left[\frac{1}{r}\frac{\partial}{\partial r}\left(r\frac{\partial \vartheta}{\partial r}\right) + \frac{\partial^2 \vartheta}{\partial z^2}\right] \tag{1}$$

where the thermal properties ρ, c and k are the material density, specific heat and thermal conductivity, respectively. The temperature field within the material $\vartheta(r, z, t)$ is to be obtained upon solving the energy equation subjected to the appropriate boundary and initial conditions. Fig. 1 displays a schematic representation of a plate with appropriate definitions. There are four types of boundary conditions: convective, insulated, symmetric, and given heat flux boundary conditions.

(i) Convective boundary conditions on the front and the rear faces of the plate which can be expressed as

$$-k\frac{\partial \vartheta}{\partial r} = h(\vartheta - \vartheta_\infty) \tag{2}$$

where h, and ϑ_∞ are the free convective heat transfer to the ambient and the ambient temperature, respectively.

(ii) Insulated boundary condition on the plate edges (side faces) is assumed since the plate dimension in radial direction, r, is quit long enough such that the heat diffusion at that edges is negligible, and can be expressed by

$$\frac{\partial \vartheta}{\partial r} = 0 \tag{3}$$

(iii) Symmetric boundary condition, $r = 0$, and is treated as the boundary condition given in (ii).

(iv) Given heat flux boundary condition at the plate center on the front face represented by the circular area of the front-face spot radius, r_0, for the arc duration time t_d, and is

expressed as

$$-k\frac{\partial \vartheta}{\partial r} = P(r,t) \quad \text{for } 0 \leqslant r \leqslant r_0 \text{ and } 0 < t \leqslant t_d \tag{4}$$

where $P(r,t)$ is the arc equivalent thermal power intensity. After the arc dies out, the same area is left bare for free convection heat transfer as given by

$$-k\frac{\partial \vartheta}{\partial r} = h(\vartheta - \vartheta_\infty) \quad \text{for } 0 \leqslant r \leqslant r_0 \text{ and } t > t_d \tag{5}$$

The transient conduction differential equation is numerically solved by the finite volume technique [17,18]. The basic principle of the finite volume technique is based on dividing the calculation domain into a number of non-overlapping control volumes such that there is only one control surface surrounding each control volume.

The grid points are numerically located in the center of the control volumes. Thereafter, the differential equation is integrated over each control volume. This integration is performed after making presumptions about the manner in which the variable ϑ is distributed between grid's nodes. It is assumed that the variable ϑ is varied in a linear manner between grid's nodes. At each time step the discretization equation leads to a system of linear algebraic equations containing the values of ϑ for grid's points. After imposing the foregoing boundary conditions in their numerical forms, the solution of the resulting system of equation is obtained. Then, the solution is advanced in time to obtain the temperature field at the next time level until reaching a pre-assigned maximum time limit. Special care is taken by using variable time increments, such that the waveform of the IC is captured during each time level of the calculations. The IC rise time is divided into 10 time intervals. This time interval is used after detecting the birth of each IC up to 1.5 of its rise time. Following each IC, the time interval is uniformly increased until the IC tails off at 1.5 of its tail time. These non-uniform time intervals guarantee that each IC in such flashes having successive impulses is numerically captured during the calculations. Prosperities of all metals were taken from [19]. For metal sheets the Joule/resistive heating and the variation of the thermal conductivity due to the fast-changing current flow in the material is negligible [20].

3. Results and discussion

An experimental simulation of the effects of lightning long-duration and impulse currents (LDC and IC) striking to metallic plates was performed by measuring the temperature profiles as a function of the rear-face coordinates every 20 ms by using a sophisticated high-speed infrared camera, having an upper temperature limit of 1200 °C [14,15]. The test sample (25×25 cm^2) is concentrically fixed on an aluminum disc (diameter = 60 cm and thickness = 10 mm). The rear-face temperature profiles as a function of the coordinates and time were measured, where the electrode-jet phenomenon and arc movement were avoided. From these results, the input power density is computed by knowing the spot radius, the cathodic/anodic potential drop and the stroke current, where it is equal to the this potential drop times the stroke current divided by the spot area.

3.1. 3-D transient-temperature distribution

Fig. 2 shows a comparison between the measured [14] and computed rear-face temperature contour maps $\vartheta_r(x, y)$ for normal steel [19] at different times due to an LDC (square-like) current with an amplitude $I = -93$ A and a duration $\Delta t =$ 325 ms. A good agreement is found between the measured and the computed $\vartheta_r(x, y)$ during heating and cooling, too. Since the major part of the absorbed energy by the sample is transferred by heat conduction to the sample rear-face. Hence, the measured rear-face temperature contour maps $\vartheta_r(x, y)$ are, to some extent, similar to those occurring on the front face but with reduced scales. These contour maps "$\vartheta_r(x, y)$" are concentric circles as observed from the front-face spots. Fig. 3 illustrates the computed transient-temperature distribution along the sample thickness $\vartheta(y, z)$ for normal steel [19], where the temperature is slowly spreading due to the very low thermal

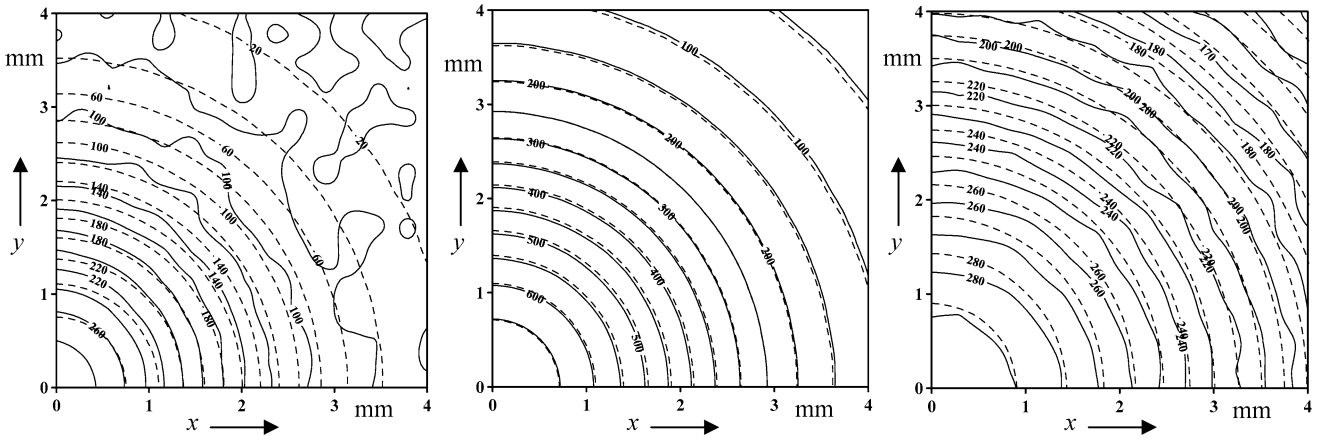

Fig. 2. Comparison between the measured (solid) and computed (dashed) rear-face temperature ϑ–r(x, y) contour maps (in °C) at different time steps for normal steel having $\delta = 2$ mm struck by an LDC of $I = -93$ A and $\Delta t = 325$ ms.

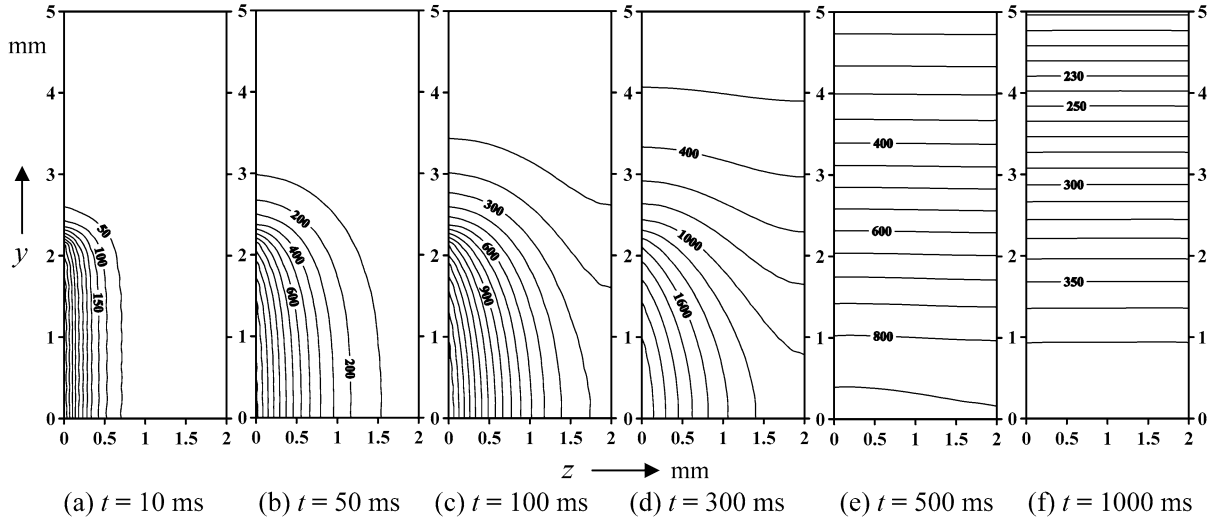

Fig. 3. Transient temperature distribution (in °C) along the sample thickness (z) for normal steel having $\delta = 2$ mm struck by an LDC of $I = -93$ A and $\Delta t = 325$ ms.

diffusivity and thermal conductivity of the steel [19], i.e. long time constant.

3.2. Injected current amplitude and sample thickness

Although the arc tends to be radially contracted at increasing the current, but it always stays symmetrical. This leads to the concentric circles of the contour maps [14,15]. Fig. 4 depicts the dependence of the rear-face maximum core-temperature (ϑ_{rm}) for aluminum sample [19] on current amplitude of LDC having $\Delta t = 525$ ms. Aluminum has a much higher thermal diffusivity and thermal conductivity than steel [19]. Therefore, ϑ_{rm} occurs just after the current quenches, i.e. short time constant. In addition, a good agreement between the measured [14] and computed ϑ_{rm} is also observed for different thicknesses of the aluminum sample. For a given current amplitude, the smaller the sample thickness the higher is ϑ_{rm}.

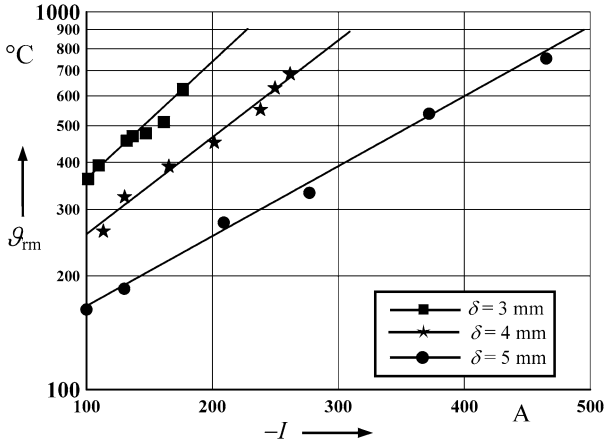

Fig. 4. Dependence of ϑ_{rm} on current amplitude of LDC ($\Delta t = 525$ ms) for aluminum sample having different δ. Lines: computed. Symbols: measured.

3.3. Impulse current (IC)

Fig. 5 shows the transient profiles of the rear-face maximum core-temperature (ϑ_{rm}) for different metals [19] having $\delta = 2$ mm struck by IC (85 kA peak, 12/550 μs), where this current represents the positive return stroke [9]. The observed trend of ϑ_{rm} may be attributed to the fact that the spot diameter in case of IC is much larger than that in case of LDC [14,15]. In case of a much smaller LDC spot diameter, high heat is dissipated sideways into the material by heat conduction. While in case of a large IC spot diameter, with almost equal heat flux over a wider area, only a small part of the heat is dissipated into the material. Here, the cooling down of the spot occurs mainly by convection/radiation into the ambient air. For metals, as it is well known, heat conduction is a much faster process than heat convection/radiation. Consequently, an LDC following a first return stroke will lead to the accumulative thermal effect, i.e. "temperature build up" as can be seen in Fig. 5. Good agreement between the measured and computed ϑ_{rm} is observed for the aluminum sample.

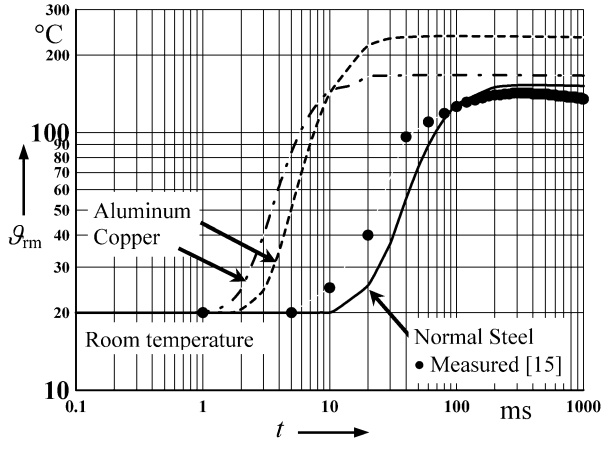

Fig. 5. Transient profiles of ϑ_{rm} for different metals having $\delta = 2$ mm struck by IC (85 kA peak, 12/550 μs) simulating the positive return stroke current.

3.4. Mixed LDC and IC for metals

The power density (P) and the current waveforms of any lightning flash are identical. Fig. 6 illustrates the simulated

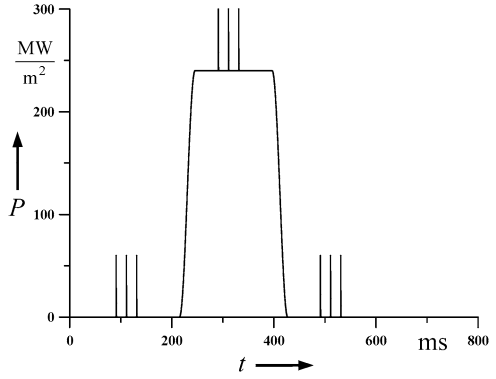

Fig. 6. Simulated power density of a lightning flash having $n = 3$ and 0.25/100 μs.

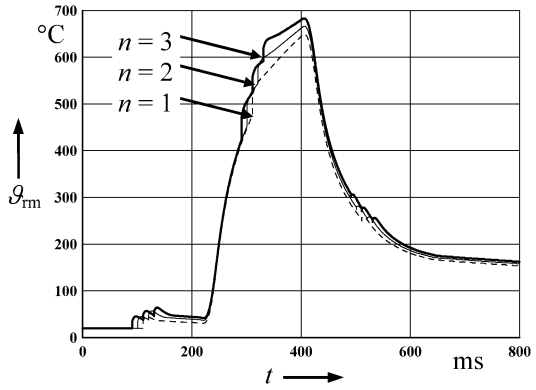

Fig. 7. Transient profiles of ϑ_{rm} for aluminum having $\delta = 2$ mm struck by the lightning flash shown in Fig. 6.

power density (P) of a given lightning flash representing the "downward flash", which consists of three impulses ($n = 3$) for each of the preceding, the superimposed on a long-duration one, and the subsequent ones. Each impulse simulates the IC having a power density $P = 60\ \mathrm{MW\,m^{-2}}$, while the ratio of the power densities simulating the LDC to that of the IC is taken as 4. The simulated power density in Fig. 6 is also chosen for simplicity reasons. It represents an artificial mixture of the following two kinds of lightning flashes when: (1) the aircraft itself triggers the lightning and (2) the aircraft intercepts a natural lightning. The front-face spot diameter is considered to be as large as 2 mm [14]. The front-face spot diameter is kept constant during such mixed current strokes.

Fig. 7 depicts the variations in the transient profiles of the rear-face maximum core-temperature (ϑ_{rm}) for aluminum. These results reveal that the transient-temperature response of aluminum is insignificantly governed by the number of the IC impulses (n). The effect of the IC is not dominant because of the short response time of the aluminum. For a constant power density of the IC, other results reveal that ϑ_{rm} show an approximate linear dependence on the relative power density (power density of LDC to that of IC). A similar trend is also observed for the case of having a constant power density of the LDC and increasing that of the IC.

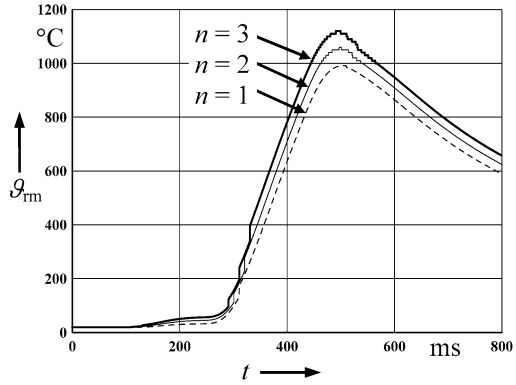

Fig. 8. Transient profiles of ϑ_{rm} for two-layer Al/C (0.1/1.9 mm) sample.

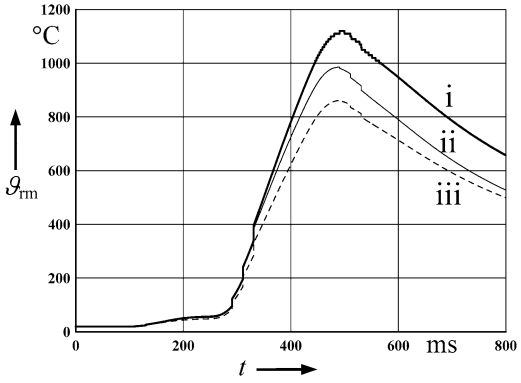

Fig. 9. ϑ_{rm} profiles for $n = 3$ and for multi-layer samples.

3.5. Mixed LDC and IC for composites

This section gives an introduction for studying the transient profiles of the rear-face maximum core-temperature (ϑ_{rm}) for samples consist of multi layers, i.e. aluminum and carbon, with an overall thickness $\delta = 2$ mm. For Figs. 7–9, it is also assumed that the front face is normally made of aluminum and struck by the same lightning flash illustrated in Fig. 6. The carbon properties are taken as $\rho = 1600\ \mathrm{kg\,m^{-3}}$, $c = 2000\ \mathrm{J\,kg^{-1}\,K^{-1}}$ and $k = 15\ \mathrm{W\,m^{-1}\,K^{-1}}$ [6].

Fig. 8 shows the transient profiles of ϑ_{rm} for various number of IC (n) and for two-layer aluminum (Al) on the front face and carbon on the rear face, where the thickness ratio of Al/C is 0.1/1.9 mm. It seems that the effect of n becomes sensible in case of such composite material because of the long time constant of the carbon as a result of its poor thermal conductivity and high specific heat. This also leads to higher ϑ_{rm} and longer time-to-peak for $\vartheta_{rm}(t)$ profiles in comparison to those of the results in Fig. 7 for pure aluminum.

Other results show that a significant damping of these profiles along the sample thickness occurs inside the carbon layer because of the above-mentioned reason. A similar trend of these results is also obtained experimentally for steel [14].

Since carbon has bad thermal properties, therefore it is of significant importance to reduce the rear-face temperature. Different samples are investigated, namely,

(i) Al/C = 0.1/1.9 mm,
(ii) Al/C/Al/C = 0.1/0.9/0.1/0.9 mm, and
(iii) Al/C/Al = 0.1/1.8/0.1 mm.

Fig. 9 illustrates the effect of adding a thin layer of aluminum either inside the carbon (configuration (ii)) or on the rear face (configuration (iii), i.e. sandwiching the carbon between two identical thin aluminum layers) with keeping the overall thickness of the sample to be constant and equal to 2 mm. The peak value of the rear-face temperature profiles is dominantly reduced by adding the above-mentioned aluminum layer, where configuration (iii) gives the highest reduction. This can be explained by the following fact. In the two cases (ii) and (iii), high heat is dissipated sideways into the material by heat conduction leading to the decrease in the transient profiles of ϑ_{rm}. Other results also reveal that there is no significant difference between case (ii) and the case Al/C = 0.2/1.8 mm. In addition, there is no appreciable effect of the IC waveform (either in the order of negative subsequent or negative first return strokes) on the rear-face core temperature for both metals and composites. The front-face "first" layer (Al = 0.1 mm) simulates the lightning protection by a mesh. The samples (ii) and (iii) are not used in aircraft skin, but they are examined just to show that it is possible to reduce the rear-face temperature without changing the sample thickness.

4. Conclusions

A computer program based on the finite volume technique is written to compute the transient-temperature distributions in the three dimensions for metals and composites struck by simulated lightning flashes. Good agreement between the measured and the computed profiles is found for striking metallic plates with both long-duration and impulse currents. Impulse currents produce much lower rear-face temperatures with prolonged profiles for a few minutes. On the contrary, long-duration currents produce higher rear-face temperatures with their profiles decay just after their generating currents die out.

The results also reveal that under mixed current flashes, the higher thermal diffusivity and thermal conductivity the lower is the prolonged temperature profiles with time even after quenching the arc. The superimposed and/or the subsequent impulse currents give an increase in the rear-face temperature, while the preceding ones do not significantly contribute to the temperature rise on the rear face. For such mixed current flashes and for metals having good thermal properties, there is a negligible effect of the number of impulse currents on the rear-face transient temperature profiles. On the contrary, for aluminum/carbon composites, this effect becomes appreciable with a delay in the occurrence of the peak value of the rear-face temperature profiles. Keeping the overall thickness constant, the addition of a thin aluminum layer to the rear face significantly reduces the rear-face temperature.

Acknowledgements

The first author wishes to acknowledge his indebtedness to both the Alexander von Humboldt Foundation for its financial support and the University of the Federal Armed Forces, Munich, Germany for its generous hospitality.

References

[1] P. Lalande, A. Bondiou-Clergerie, P. Laroche, Analysis of available in-flight measurements of lightning strikes to aircraft, in: Int. Conf. on Lightning a. Static Electricity, France, 1999, pp. 401–408.
[2] EUROCAE, Aircraft Lightning Environment and Related Test Waveforms Standard, EUROCAE ED-84 WG-31/SAE AE4L, Paris, France, 1997.
[3] A.J. Eriksson, The incidence of lightning strikes to power lines, IEEE Trans. Power Delivery 2 (3) (1987) 859–870.
[4] A. Larsson, P. Lalande, A. Bondiou-Clergerie, A. Delannoy, The lightning swept stroke along an aircraft in flight. Part I: Thermodynamic and electric properties of lightning arc channels, J. Phys. D: Appl. Phys. 33 (2000) 1866–1875.
[5] A. Castellani, A. Bondiou-Clergerie, P. Lalande, A. Bonamy, I. Gallimberti, Laboratory study of the bi-leader process from an electrically floating conductor. Part I: General results, IEE Proc.-Sic. Meas. Technol. 145 (5) (1998) 185–192.
[6] F.A. Fisher, J.A. Plummer, R.A. Perala, Aircraft Lightning Protection Handbook, Report DOT/FAA/CT-89/22, Federal Aviation Administration Technical Center, Atlantic City/USA, 1989 (Chapters 3, 4, 6 and 8).
[7] K.E. Crouch, Minimum ignition levels of aircraft fuel constituents to lightning related ignition sources, in: Int. Conf. on Lightning Static Electricity, Dayton, USA, 1986, Proc., pp. 48-1–48-17.
[8] M.A. Uman, The Lightning Discharge, Academic Press, Florida, USA, 1987 (Chapters 2 and 14).
[9] K. Berger, Novel observations on lightning discharges: results of research on mount San Salvatore, J. Franklin Instit. 283 (6) (1967) 478–525.
[10] F. Heidler, W. Zischank, J. Wiesinger, Statistics of lightning current parameters and related nearby magnetic fields measured at the Peissenberg tower, in: Int. Conf. on Lightning Protection, Greece, 2000, Paper 8.9, pp. 78–83.
[11] B.W. James, G.H. Wostenholm, G.S. Keen, S.D. McIvor, Prediction and measurement of the thermal conductivity of composite materials, J. Phys. D: Appl. Phys. 20 (1987) 261–268.
[12] T. Ford, Aerospace composites, Aircraft Engrg. Aerospace Technol. 69 (4) (1997) 334–342.
[13] A. Vlot, L.B. Vogelesang, T. de Vries, Towards application of fiber metal laminates in large aircraft, Aircraft Engrg. Aerospace Technol. 71 (6) (1999) 558–570.
[14] I.A. Metwally, F. Heidler, W. Zischank, Measurement of the rear-face temperature of metals struck by lightning long-duration currents, European Trans. Electrical Power 14 (4) (2004) 201–222.
[15] I.A. Metwally, F. Heidler, W. Zischank, Factors influencing the surface-temperature rise of metals exposed to different lightning currents, in: Int. Conf. Lightning Protection, Cracow, Poland, 2002, pp. 779–784.
[16] P.F. Incropera, P.D. DeWitt, Introduction to Heat Transfer, Wiley, New York, 1996.
[17] S.V. Patankar, Numerical Heat Transfer and Fluid Flow, Hemisphere Publishing Corporation, Taylor & Francis Group, New York, 1980.
[18] M. Peric, R. Kessler, G. Scheuerer, Comparison of finite-volume numerical methods with staggered and co-located grids, Comput. Fluids 4 (1988) 389–403.
[19] M. Necati Özişik, Heat Transfer: A Basic Approach, first ed., McGraw-Hill Book, New York, 1985.
[20] Ph. Testé, T. Leblanc, F. Uhlig, J.-P. Chabrerie, 3D modeling of the heating of a metal sheet by a moving arc: Application to aircraft lightning protection, Eur. Phys. J. AP 11 (2000) 197–204.